Journal of the Korean Nuclear Society
Volume 28, Number 2, April 1996

Multi-phase Flow Modeling of Vapor Explosion Propagation

I.K. Park and G.C. Park
Seoul National University
K.H. Bang*
Pohang University of Science and Technology
(Received July 21, 1995)

증기폭발 전파과정 해석을 위한 다상유동 모델 개발

박익규 · 박군철
서울대학교
방광현*
포항공과대학교
(1995. 7. 21 접수)

Abstract

A mathematical model of vapor explosion propagation is presented. The model predicts two-dimensional, transient flow fields and energies of the four fluid phases of melt drop, fragmented debris, liquid coolant, and vapor coolant by solving a set of governing equations with the relevant constitutive relations. These relations include melt fragmentation, coolant phase-change, and heat and momentum exchange models. To allow thermodynamic non-equilibrium between the coolant liquid and vapor, an equation of state for water is uniquely formulated. A multiphase code, TRACER, has been developed based on this mathematical formulation. A set of base calculations for tin/water explosions show that the model predicts the explosion propagation speed and peak pressure in a reasonable degree although the quantitative agreement relies strongly on the parameters in the con stitutive relations. A set of calculations for sensitivity studies on these parameters have identified the important initial conditions and relations. These are melt fragmentation rate, momentum exchange function, heat transfer function and coolant phase change model as well as local vapor fractions and fuel fractions.

요 약

본 논문에서는 증기폭발의 전파과정을 해석하기 위한 수학적 모델을 제시하였다. 이 모델은 용융물, 용융파편, 그리고 냉각재 기상과 액상 등 4상 유체의 2차원적인 천이거동을 지배방정식 및 관련상관식의 수치적 해를 구함으로서 예측할 수 있다. 모델에 사용된 주요 상관식은 용융물 분쇄, 냉각재 상변화, 에너지 교환, 그리고 운동량 교환항으로 구성되어 있다. 그리고, 냉각재(물)의 상태방정식은 냉각재의 기상과 액상 사이의 열역학적인 비평형을 허용할 수 있는 독특한 형태로 구성되었다. 주석/물의 증기폭발에 대한 예제계산을 수행한 결과 본 모델이 폭발의 전파속도 및 압력 -비록 그 정량적인 값은 관련상관

* Current Address : 한국원자력연구소(Korea Atomic Energy Research Institute)

식의 인자들에 좌우되지마는- 등의 증기폭발 전파과정의 주요현상을 적절히 모사할 수 있음을 알 수 있었다. 또한 중요한 초기변수(증기 분율, 용융물 분율) 및 관련상관식에 대한 민감도 분석도 수행되었다.

1. Introduction

Vapor explosions or thermal detonations are the result of rapid heat transfer from a hot liquid(fuel melt) to a cooler volatile liquid(coolant) in some circumstances. Such explosions have been observed in the industrial processes where the hot melt may be contacted with the volatile fluid, e.g., the metal casting industry[1] and the paper industry[2], and in the liquified natural gas transportation[3]. Also this phenomenon may occur in the volcanic activity by the reaction between magma and sea water or underground water[4, 5].

Vapor explosions also have been paid attention in nuclear industry as the consequence of the molten core material(corium) contacting residual coolant[6] in severe accidents. This would threaten the safety directly and/or indirectly in nuclear power plants.

On the basis of the available experimental observations, it was postulated that large scale vapor explosions progress through the four distinct phases[6]; premixing, triggering, propagation, and expansion.

Board and Hall suggested that the propagation step in a vapor explosion is analogous to a chemical detonation[7]. Their model was very idealized and predicted pressures and propagation speeds much higher than those to be observed in experiments. However, their framework was a significant step forward in the understanding of the vapor explosion process.

And, Sharon and Bankoff[8] developed a steady state multi-phase flow model. Their model allows detailed investigation of the effect of rate limited processes such as fragmentation and heat transfer.

Carachalios et al.[9] developed the transient model using the shock fitting methods. In most other cases shock capturing method(multi-field modeling) has been employed.

Medhekar et al.[10] have developed a two-dimensional, transient, two-fluid model to simulate the propagation stage, given a specified triggering event. The water and steam were allowed to have each energy equation and to have different temperatures.

Fletcher[11] has developed a one-dimensional model. The model predicts that propagating detonations are possible in highly voided mixtures and that mixture inhomogeneities in one-dimension do not prevent propagation.

Young[12] has developed an integrated fuel-coolant interaction(FCI) model. This model is transient, two-dimensional and four- components descriptions of molten corium, solid corium, liquid coolant, and vapor coolant.

Corradini et al.[13, 14] have developed a model for the mixing stage and have extended the model to simulate detonations. Their model is transient, one-dimensional with two Eulerian fields(liquid water and steam) and one Lagrangian field(melt).

As noted above in the review of the past efforts on mathematical simulation of vapor explosion propagation, the four phases of fluid elements such as melt drops and fragmented debris, coolant liquid and vapor are often modeled individually. Such approaches have been successful in the mathematical point of view. However, there has been a major shortcoming in adequately describing the transport of mass, momentum and energy between these phases. Such transport phenomena include melt fragmentation, heat transfer and momentum transfer in multi-phase flow, and evaporation and condensation in highly transient and non-equilibrium flow field. An adequate set of equations of state, particularly of water, are also required.

The major reason for the deficiency in such constitutive relations is mainly due to the lack of understanding the key physical phenomena as well as experimental data and properly formulated correlations. However, one also notes that there is a limit in

obtaining a necessary set of experimental data due to the difficulties in conducting experiments of such highly transient, multi-phase phenomena. Therefore, it is necessary to identify the degree of significance of the uncertainty in each constitutive relation and to focus the effort on the major phenomena identified.

In this paper the formulation of two-dimensional, transient, multi-phase flow of vapor explosion propagation is presented. A multi-phase code, TRACER, has been developed for numerical solutions and the results of sensitivity studies on the major constitutive relations are discussed. Also the effect of the present formulation of the equation of state of water is evaluated.

2. Mathematical Models

2.1. Model Description

In the event that hot melt pours into coolant, it is postulated that fuel droplets are dispersed into coolant liquid and the vapor film exists between the hot melt and the coolant liquid. As a shock wave propagates through the premixture, melt(fuel) droplets are fragmented into fine debris and rapid heat transfer from melt to coolant occurs.

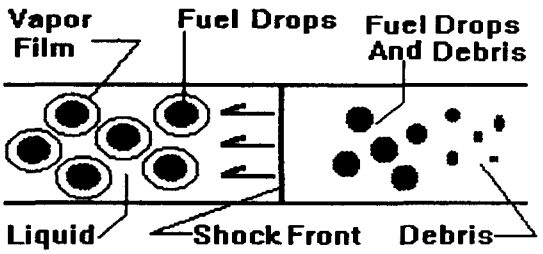

M/F	α_f	α_v	α_l	α_f	α_{db}	α_v	α_l
V/F	α_f	$\alpha_c=\alpha_v+\alpha_l$		α_f	$\alpha_c=\alpha_v+\alpha_l+\alpha_{db}$		
S/A	$\alpha_f+\alpha_v+\alpha_l=1$			$\alpha_f+\alpha_v+\alpha_l+\alpha_{db}=1$			
S/V	Premixture			Propagation			

M/F = Material Fields
V/F = Velocity Fields
S/A = Sum of All Volume Fractions
S/V = Stage of Vapor Explosions

Fig. 1. Concept of Vapor Explosions

Mixture definition is represented as the volume fraction of each fluid element. Before the shock front, the mixture consists of fuel droplets, liquid coolant, and vapor coolant. Behind the shock front the fuel droplets are fragmented by relative velocity between the fuel and coolant and the mixture is then composed of fuel droplets, liquid coolant, vapor coolant, and fine debris. Therefore, the model includes four fluid phases; fuel melt, liquid and vapor coolant, and fine debris(Figure 1). However, the combination of liquid and vapor coolant, debris is treated as one velocity field called the coolant field.

2.2. Assumptions

1) Liquid coolant, vapor and debris have same velocity. In facts, their velocities can be different each other, but under the high velocity and high pressure it is a reasonable approximation that the small debris particles move together with the coolant. This assumption make it convenient and mathematically clear that the momentum exchange and fragmentation model are introduced in the conservation equations.

2) The debris comes into local thermal equilibrium with the liquid coolant instantaneously. In real FCI debris may heat coolant liquid and vapor by some heat transfer rate. But, because this heat transfer phenomena is not quantitatively clear and vapor may be collapsed near the shock front, this assumption can be acceptable. And then, it is not necessary to specify the size of debris.

3) The temperature of fuel droplets can be assumed constant because the heat transfer rate from fuel to coolant could be rather slow compared to the propagation speed and the heat transfer rate from debris to coolant. All the heat transferred from fuel melt is added in liquid coolant, but if no liquid, in vapor coolant.

4) Boiling or condensation occur for maintaining local thermodynamic equilibrium. This concept is introduced by Medhekar et al.[10], but their results

did not show a certain evidence of thermodynamic equilibrium. And the boiling and condensation mode allows water to lie in the thermodynamic non-equilibrium state, for which the equation of state(EOS) must be carefully treated.

2.3. Conservation Equations

Conservation of mass applied to each component gives

$$\frac{\partial \alpha_f \rho_f}{\partial t} + \nabla \cdot (\alpha_f \rho_f \vec{u_f}) = -F_r \quad (1)$$

$$\frac{\partial \alpha_{db} \rho_{db}}{\partial t} + \nabla \cdot (\alpha_{db} \rho_{db} \vec{u_c}) = F_r \quad (2)$$

$$\frac{\partial \alpha_v \rho_v}{\partial t} + \nabla \cdot (\alpha_v \rho_v \vec{u_c}) = -J_e + J_c \quad (3)$$

$$\frac{\partial \alpha_l \rho_l}{\partial t} + \nabla \cdot (\alpha_l \rho_l \vec{u_c}) = J_e - J_c \quad (4)$$

where, F_r, J_e, and J_c are mass exchange rates due to fragmentation, evaporation, condensation respectively and are specified later.

Conservation of momentum for coolant and fuel gives

$$\frac{\partial (\alpha_c \rho_c \vec{u_c})}{\partial t} + \nabla \cdot (\alpha_c \rho_c \vec{u_c} \vec{u_c}) = -\alpha_c \nabla p - K(\vec{u_c} - \vec{u_f}) + F_r \vec{u_f} \quad (5)$$

$$\frac{\partial (\alpha_f \rho_f \vec{u_f})}{\partial t} + \nabla \cdot (\alpha_f \rho_f \vec{u_f} \vec{u_f}) = -\alpha_f \nabla p + K(\vec{u_c} - \vec{u_f}) - F_r \vec{u_f} \quad (6)$$

where, $\rho_c = (\alpha_l \rho_l + \alpha_v \rho_v + \alpha_{db} \rho_{db})/\alpha_c$

$\alpha_c = \alpha_l + \alpha_v + \alpha_{db}$

Right hand side represents momentum exchange due to drag and mass transfer. K is the momentum exchange function and is specified later.

Energy conservation equations are formulated in terms of internal energy and are given for liquid coolant, vapor coolant, and debris as

$$\frac{\partial (\alpha_l \rho_l I_l)}{\partial t} + \nabla \cdot (\alpha_l \rho_l I_l \vec{u_c}) + p\left\{\frac{\partial}{\partial t}\alpha_l + \nabla \cdot [\alpha_l \vec{u_c}]\right\} = -(J_e - J_c) H_v + \delta(\alpha_l) F_r H_f + \delta(\alpha_l) R_{fc}(T_f - T_l) - R_{vl}(T_l - T_v) \quad (7)$$

$$\frac{\partial (\alpha_v \rho_v I_v)}{\partial t} + \nabla \cdot (\alpha_v \rho_v I_v \vec{u_c}) + p\left\{\frac{\partial}{\partial t}\alpha_v + \nabla \cdot [\alpha_v \vec{u_c}]\right\} = +(J_e - J_c) H_v + [1 - \delta(\alpha_l)] F_r H_f + [1 - \delta(\alpha_l)] R_{fc}(T_f - T_v) + R_{vl}(T_l - T_v) \quad (8)$$

$$T_{db} = \delta(\alpha_l) T_l + [1 - \delta(\alpha_l)] T_v \quad (9)$$

where, $H_f = \left(\frac{p}{\rho_f} + I_f\right)$

$H_v = \left(\frac{p}{\rho_v} + I_v\right)$

In multi-phase flow the surface area per unit volume of the interpenetrating phases plays an important role in determining interfacial drag and heat transfer. A transport model of the interfacial area was developed by Ishii[16], assuming the melt is composed of spherical droplets. The resulting equation for the diameter of the fuel droplets is given by

$$\alpha_f \rho_f \frac{\partial L_f}{\partial t} + \alpha_f \rho_f \vec{u_f} \nabla \cdot L_f = -F_{rag} \quad (10)$$

The right-hand side of the equation arises as a consequence of the mass loss due to fragmentation.

In addition to the above equation there is the volume constraint that

$$\alpha_f + \alpha_l + \alpha_v + \alpha_{db} = 1 \quad (11)$$

These complete the specification of the differential equations. The next sections contain the description of constitutive relations used to close the model, the equations of state (EOS), and the boundary and initial conditions.

2.4. Constitutive Equations

In this section the constitutive relations for heat transfer, momentum exchange, and fragmentation employed in the model are described. These constitutive relations have been generally applied in vapor explosion models, but their validity and usefulness must be investigated individually and/or mutually. In this paper sensitivity studies for these constitutive relations are presented and their appropriateness is discussed.

2.4.1. Heat Transfer Functions

Interfacial heat transfer from the fuel droplets to the coolant is through the convection(film boiling) and radiation mechanism. The heat transfer coefficient, R_{fc}, is determined by their superpositions and Medhekar et al.[10] suggested the formulation as

$$R_{fc}= n_f(h_r+h_c)4\pi r^2(1-\varepsilon_v) \tag{12}$$

where, $n_f= \frac{3}{4}\frac{\alpha_f}{\pi r^3}$

$$h_r= \sigma E_f \frac{T_f^4-T_l^4}{T_f-T_l}$$

$$h_c= 2.98\{\rho_v k_v[I_{vl}+0.68c_{pv}(T_f-T_l)]\} *\{|\overrightarrow{u_f}-\overrightarrow{u_l}|/2r_f(T_f-T_l)\}$$

The heat transfer from fuel melt to coolant can be neglected with compared to the heat from debris. In this paper, the use of heat transfer function is retained.

Heat transfer between the liquid coolant and vapor is not modeled, but for investigating its effects on explosion phenomena and also on thermodynamic equilibrium of the coolant a constant value is introduced in the region of

$$R_{vl} = 0 \sim 10^{11} W/m^2K \tag{13}$$

2.4.2. Momentum Exchange Functions

Medhekar et al.[10] used the interfacial momentum exchange function between the fuel droplet and the coolant given below. The interfacial momentum exchange function, K, consists of two terms. The first represents the drag arising from the relative velocity. The second term accounts for the added mass effect, which may be important during the sudden acceleration induced by the passage of shock wave. The function is given as

$$K= \frac{3}{8}\frac{C_D\alpha_f\alpha_c\rho_c|\overrightarrow{u_c}-\overrightarrow{u_f}|}{r_f} + \frac{1}{|\overrightarrow{u_c}-\overrightarrow{u_f}|}\alpha_v\rho_v\left|\frac{d(\overrightarrow{u_c}-\overrightarrow{u_f})}{dt}\right| \tag{14}$$

2.4.3. Phase Change Functions

Within the coolant field phase changes are taken at rates appropriate to maintain the liquid and vapor phases in local thermodynamic equilibrium. If desirable, a non-equilibrium state could also be accommodated by appropriate alternative formulations for the phase change.

However, no appropriate model exists for this non-equilibrium state. In the framework of two-fluid modeling this can be accomplished by specifying adequately high evaporation or condensation rates, while avoiding overshoots and maintaining stability in the computation. Medhekar et al.[10] suggested the formulation as

$$J_e = \frac{\alpha_l\rho_l}{\tau}\left[\left(\frac{p_s}{p}\right)^{1/\gamma}-1\right] \tag{15}$$

$$J_c = \frac{\alpha_v\rho_v}{\tau}\left[1-\left(\frac{p_s}{p}\right)^{1/\gamma}\right] \tag{16}$$

where τ is used as an appropriately specified relaxation time.

They reported that their results are insensitive to the choice of τ in the range from 0.1 to 10 ms and the best results were obtained when τ was set equal to the time step-typically 1 ms. But, there is no proof for this phase change model to maintain appropriate thermodynamic equilibrium in their results. Okano

[15] used this phase change model together with large heat transfer coefficient between the liquid coolant and vapor to maintain the thermodynamic equilibrium of the coolant.

2.4.4. Fragmentation Rate

Fletcher[11] introduced a fragmentation model based upon boundary layer stripping due to the relative velocity.

$$F_r = c_{frag}\alpha_f |\vec{u_f} - \vec{u_c}| \pi L_f^2 \sqrt{\rho_f \rho_c / L_f} \quad (17)$$

In his calculation c_{frag} was set equal to 1.0. In this paper, the sensitivity on c_{frag} (0.5~2.0) is investigated. Since the diameter changes of fuel droplets are equal to 1/3 the rate of its volume, the source term in equation (10) is given

$$F_{rag} = \frac{1}{3} F_r L_f \quad (18)$$

2.5. Equations of State (EOS)

For water, EOS is constructed based upon NBS/NRC steam tables[17]. However, thermodynamic non-equilibrium data is required under the current phase change model, which is resulted from the separate coolant energy equations. The liquid coolant and vapor always move from non-equilibrium state to equilibrium state through the phase change.

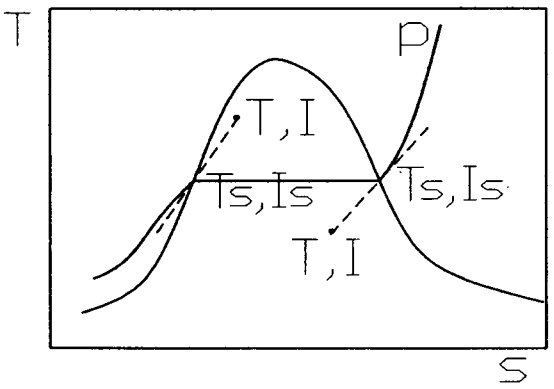

Fig. 2. Concept Diagram of Water EOS

Therefore, the superheated liquid and supersaturated vapor, which dotted line in Figure 2, must be allowed and these states are as follow.

1) To determine the saturation temperature and liquid and vapor internal energies and densities (T_s, I_{ls}, I_{us}, ρ_{ls}, ρ_{us}) under the current pressure p.

2) To calculate each current temperature(T_l, T_v) using T_s, C_p, I_l, I_v as

$$T_l = T_s(p) + (I_l - I_{ls}(p))/C_{pl}(p) \quad (19)$$

$$T_v = T_s(p) + (I_v - I_{us}(p))/C_{pv}(p) \quad (20)$$

3) To calculate the vapor and liquid densities through temperature correction with the saturation density at current pressure p and pressure correction with the saturation density at current temperature T.

$$\rho_l(p, T_l) = \rho_{ls}(T_l) + \frac{\rho_{ls}(T_l)}{E}[p - p_s(T_l)] \quad (21)$$

$$\rho_v(p, T_v) = \rho_{us}(p)\left(\frac{T_v}{T_s(p)}\right) \quad (22)$$

where E is Bulk Modulus of water and is assumed constant($E = 2.19 * 10^3$ *MPa*)

The above procedure is not exactly correct but the best in treating our separated coolant energy equations and phase change models. EOS methodology to admit thermodynamic nonequilibrium must be continuously studied in the future.

Fuel droplets and fragments are incompressible and therefore, fuel and debris densities are constant. At this general assumption in vapor explosion models, it is simple to determine the thermodynamic states of fuel melt and debris.

2.6. Boundary and Initial Conditions

The above equations are solved in a solution domain which represents an initial mixture contained in a closed vessel. Thus, the only boundary condition needed is to set the normal velocities or the all-components velocities to zero at the vessel walls. The in-

itial conditions are required for the volume fractions, velocities, temperatures and particle size distribution.

3. Numerical Procedure

A multiphase code, named as TRACER(TRAnsient Computation of Explosive Reactions), has been developed based on above mathematical formulation. The numerical scheme used for the code is based on the ICE technique. The conservation equations described earlier are written in finite-difference forms using the partial donor cell differencing for calculation of the convective fluxes. The resulting finite difference equations, which are fully implicit in the exchanges of mass, momentum, and energy, are solved by a point relaxation technique without linearization. An outline of solution scheme, which is developed on the basis of the K-FIX code[18], is as follows.

Each cycle begins with the field variables as computed in the previous cycle, or specified as initial conditions.

1) The momentum density functions are calculated from the momentum equations by accounting for only momentum convection leading to advanced time estimates of velocity and mass fluxes.

2) Advanced time estimates of the exchange functions(the interfacial heat transfer, the fragmentation rate, momentum exchange, and the boiling/condensation rates) and the advanced time mass flux are computed.

3) An iteratively implicit numerical solution is then obtained by iteration on the pressure, using a constrained two-sided Secant method such that the discrepancy in the mass conservation equations are brought down to an acceptable level (convergence criterion, $|(\alpha_l\rho_l)^{n+1}-(\alpha_l\rho_l)^n| < 1.E\text{-}7$ or $|(\alpha_g\rho_g)^{n+1}(\alpha_g\rho_g)^n| < 1.E\text{-}4$). This involves the implicit solution of the fuel, coolant liquid and vapor, and debris continuity equations. Densities and temperatures are evaluated from the respective equations of state. This iterative scheme also contains the calculation of internal energy omitting temporarily the effects of convection, work, and single-phase conduction.

4) Once the iterations are completed, new values of internal energies containing the effects of convection, work, and single-phase conduction are calculated and then new temperatures are evaluated. Now, these values are used in next time step calculation.

4. Results and Discussion

The present model is two-dimensional, but all calculations were performed for one-dimensional shock tube, which is a typical geometry of tin/water experiments. The shock tube is 1.5m long and each mesh is 0.01m. In all calculations the time step is typically $10\mu s$, which is an appropriate value because in this calculation the explosion propagation speed is about 100~500m/sec. The initial conditions and key parameters are summarized in Table 1, in which (A) is a base case condition and (B) is a overall condition based upon Baines[19] experiments with tin/water.

The calculations are started by triggering at special mesh of the initial premixture of the initialized premixture. Triggering is initiated by specifying the high pressure in the cell. Medhekar et al.[10] initiated triggering events by specifying the large fragmentation rate in cell No 1. In the initial stage of vapor explosions, fragmentation is more likely to be dominated by

Table 1. Initial Conditions for Explosions

System	Tin/Water (A)	Tin/Water (B)
Pressure(MPa)	0.1	0.1
Fuel Temperature(K)	1123	1123
Water Temperature(K)	373	373
Fuel Volume Fraction	0.4	0.2
Void Fraction	0.1	0.2
Fuel Radius(m)	0.005	0.005
Time Step(musec)	0.1	0.1
τ (msec)	1.0	1.0
c_{frag}	1.0	1.0
C_D	2.0	2.0
$R_{wl}(Wm^{-2}K^{-1})$	0.0	0.0

thermal effects or transient boiling than by hydrodynamic effects. And the detailed physics of the triggering is certainly not reflected in the formulation for fragmentation utilized at present. Thus, these initiating events are arbitrary quantities and are researchers' choices because the detailed triggering event has not been identified and the propagation may be not affected by the details of the triggering.

4.1. Base Calculations

The calculated escalation/propagation processes for the case (A) in Table 1 are shown in Figure 3. The figure represents the pressure and fragmentation rate by the time interval of 1.0ms and velocities, temperatures, droplet diameter, and volume fractions at 5.0ms as a function of space.

As the figure, pressure profiles well show the escalation/propagation process of the shock wave in vap-

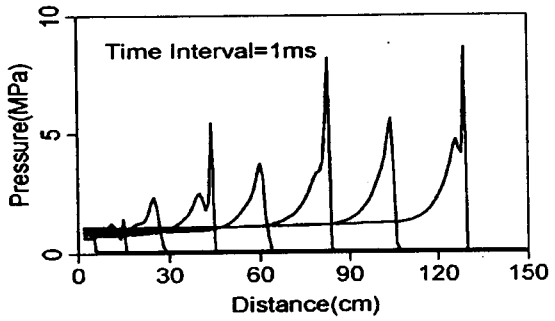

Fig. 3-a. Pressure Profiles per 1ms

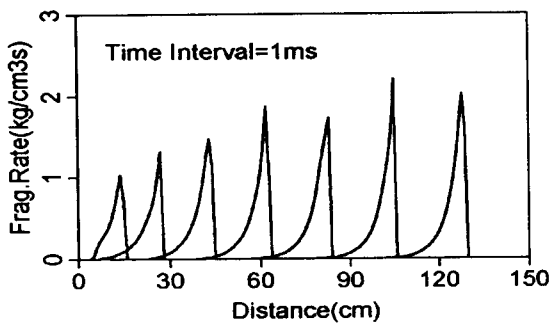

Fig. 3-b. Fragmentation Rates per 1ms

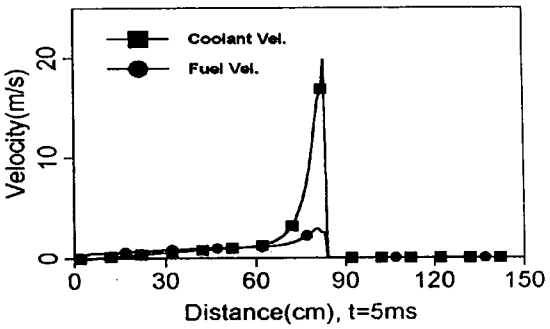

Fig. 3-c. Velocities Profiles at t=5ms

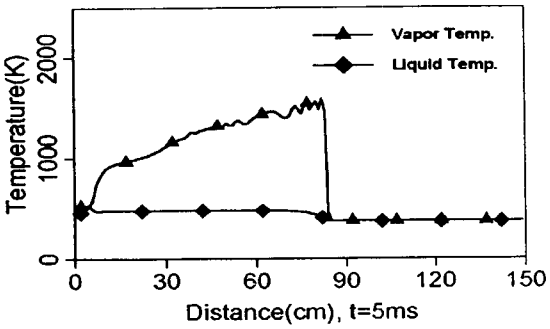

Fig. 3-d. Temperatures Profiles at t=5ms

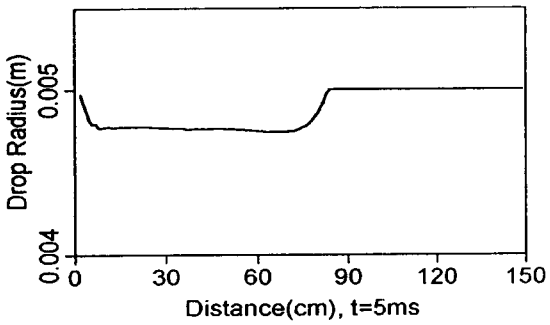

Fig. 3-e. Drop Radius Profile at t=5ms

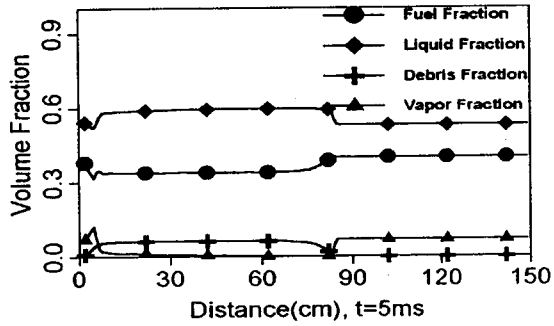

Fig. 3-f. Volume Fractions at t=5ms

Fig. 3. Base Case Results with Table 1(A)

or explosions. The peak pressure does not steadily increase. This may be caused by the instability due to the highly thermodynamic non-equilibrium of the liquid and vapor coolants and will discussed later. In this case, average explosion propagation speed($\bar{V}_{prop}$) is about 200m/sec.

Fragmentation rate profiles show a good consistency with the pressure profiles. The present model employs the hydrodynamic fragmentation mechanism by the relative velocity between coolant and fuel. The figure also presents the velocities of the coolant and fuel when time of 5ms is elapsed.

The fragmentation rate and the velocities profiles maintain physical consistency each other. The relative velocity becomes zero at 30cm behind the shock front and no fragmentation. If the fragmentation rate increases, the fragmentation zone is narrower because the large fragmentation rate results in the relative velocity become rapidly down. This rapid down of the relative velocity may be induced by following reasons ; the rapid decrease of fuel droplet size and coolant velocity due to the large fragmentation rate and the increase of debris mass add into coolant.

The diameter of fuel droplets decreases following as the fragmentation process behind the shock front. The region in which the diameter decreases, is corresponding to the fragmentation zone. The drop diameter profiles and fragmentation rate profiles in the figure show well this process.

Temperatures profiles do not show that the liquid coolant and vapor exist in thermal equilibrium state but that their states become in equilibrium. At the shock front vapor temperature is very high and decreases as the mixture is going far from the front. This high vapor temperature may be induced by the compression of vapor under the high pressure or the highly non-equilibrium. The highly non-equilibrium will give limitation to our EOS believed to be used near saturated state and be discussed later.

Volume fractions of four-phases are also presented at the figure. Before the shock front the volume fractions maintains initial mixture compositions. When the shock front arrived at mixture, the volume fractions are increased or decreased due to the compression, phase change and fragmentation. Behind the shock front major phenomena are vapor collapse and the fragmentation and these are resulted in the decrease of vapor fraction and the increase of debris fraction. Also the liquid coolant fractions and the fuel fractions surfer contrary phenomena to maintain mass conservation.

4.2. Comparison with Baines' Experiments

The calculation using the initial conditions of Table 1(B) based upon Baines experiments, are also performed. Baines' test section is ~1.0m long tube with the diameter of 29.5mm. The test section were filled with hot water of which the temperature is ~90°C. The water in the triggering section, which located in the bottom of the test section, remained cold, typically ~20°C. The experiments were started with pouring the melt from upper part of test section. When the poured melt arrived in the triggering section, the melt fragmented into debris due to some thermal effect.

In this paper, the initial conditions in the Table 1 (B) are used to calculate the CT16 test. The calculated escalation/propagation processes for the condition are shown in Figure 4. The figure represents the pressure and fragmentation rate by the time interval of 5.0ms and velocities, temperatures, droplet diameter, and volume fractions at 5.0ms as a function of space.

The calculated peak pressure and average propagation speed are ~3.0MPa and ~100m/s, respectively. The velocities, temperatures, and volume fractions are all lower than the calculated results for Table 1(A) case. But, the fuel droplet radius largely decreases than (A) case due to the late propagation. These results are physically acceptable with considering the large void fraction and the small fuel fraction than those of (A) case.

In CT16 test of the experimental series, the peak

pressure and average propagation speed are 2.5~3.5MPa and 70~180m/s, respectively. The resulted experimental pressure profiles are shown in Figure 5. The pressure profile were recorded by pressure transducers numbered T1 to T4 in order from the bottom of the test section with the interval of ~25cm.

The calculated propagation speed and peak pressure are in acceptable agreement with the experimental results. However, the experimental pressure profiles of Figure 5 show the relatively steady propagation with the pressure of 2.5~3.5MPa, but the numerical results of Figure 4 shows that the explosion pressure continuously grows from 1.0 to 3.0 MPa.

Here, we must note that the current initial volume fractions(fuel and void fraction) are assumed values

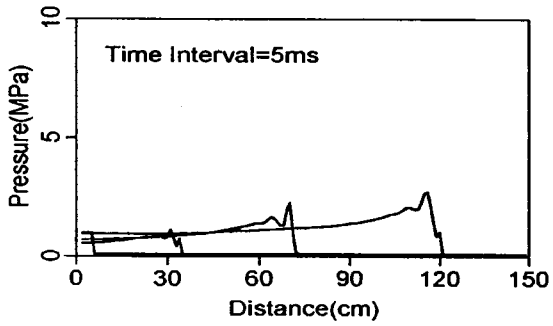

Fig. 4-a. Pressure Profiles per 5ms

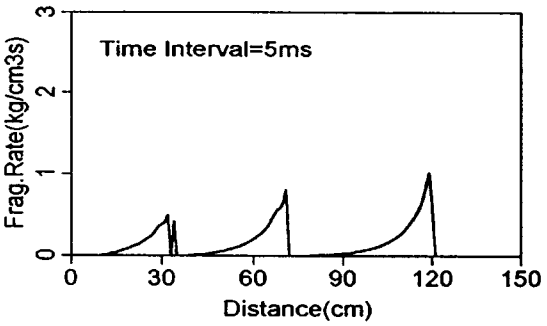

Fig. 4-b. Fragmentation Profiles per 5ms

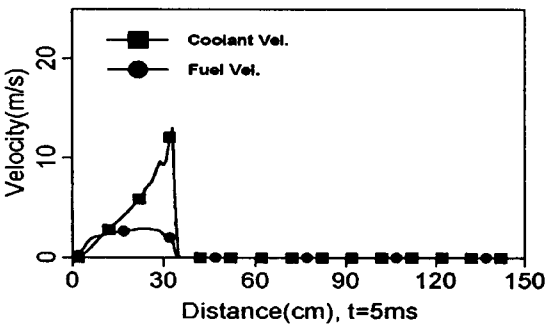

Fig. 4-c. Velocities Profiles at t=5ms

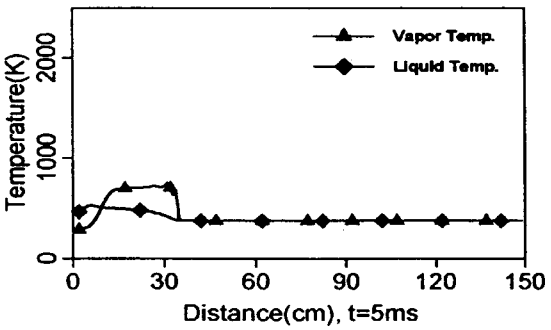

Fig. 4-d. Temperatures Profiles at t=5ms

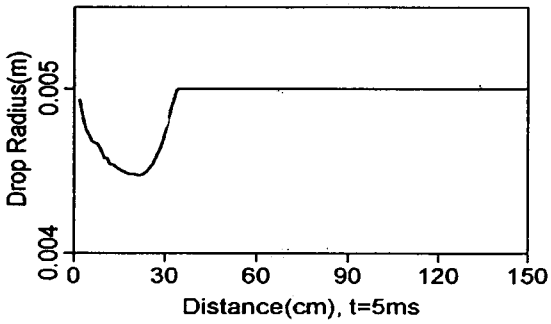

Fig. 4-e. Drop Radius Profile at t=5ms

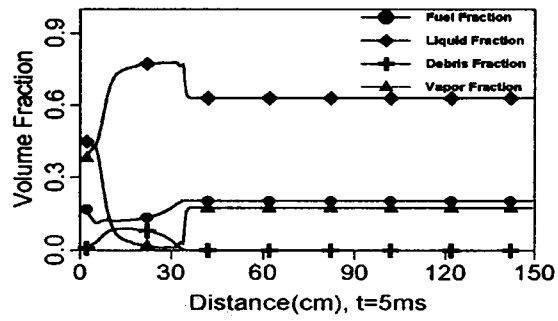

Fig. 4-f. Volume Fractions at t=5ms

Fig. 4. Calculation Results with Table 1(B)

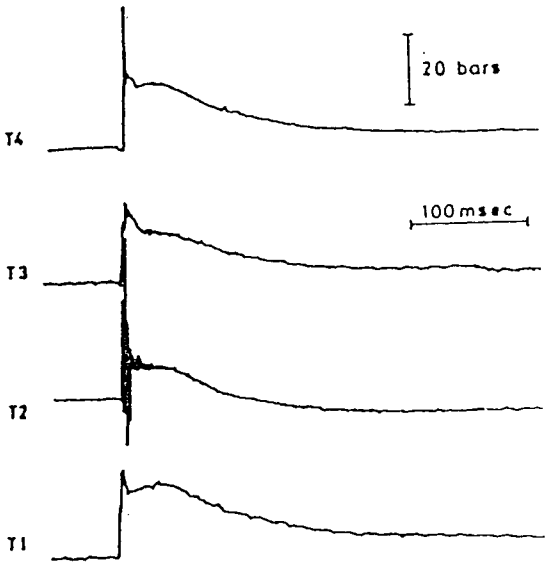

Fig. 5. Pressure Profiles in CT16[19]

because the exact mixture condition cannot have been measured and only overall fractions can be estimated. Also, the reported overall fractions must contain some uncertainties, for example, void fraction may be concentrated in the upper section and fuel fraction may be higher in the lower section. Thus, the experimental results show that the propagation speed decreases in the upper part; 130, 180, 70m/s in T1~T2, T2~T3, T3~T4.

In this point, the Table 1(A) condition can be used for the numerical calculations with locally concentrated mixture. The results(Figure 3) with this condition with compared to the experimental value in peak pressure and propagation speed(8MPa, 200m/s), but the steady propagation behaviors can be shown.

The discrepancy between the numerical and experimental results, also can be attributed to the uncertainties of the current constitutive models as well as the initial mixture fraction. These uncertainties will be evaluated in the sensitivity study of the next section.

4.3. Sensitivity Studies

A series of calculations based upon Table 1(A),

Table 2. Explosion Pressure and Propagation Speed Upon Various Values of Selected Parameters(N Represents no Explosion Propagation, and * is Base Value)

Parameter	Initial Value	P_{peak}(MPa)	$\bar{V}_{peop}$(m/sec)
ε_v	.05 .1* .2 .3	N 8 6 4	N 200 120 80
α_f	.2 .3 .4* .45	N N 8 N	N N 200 N
C_{frag}	.5 1.* 2.	N 6 15	N 200 500
R_{bl}	.0* 10^3 10^7 10^{11}	8 10 13 N	200 200 200 N
τ	.1 .5 1.* 10.	N 7 8 9	N 200 200 200
C_D	1. 2.* 4.	10 8 5	250 200 150

When initial void fraction, ε_v, changes from 0.1 to 0.3 and other conditions do not change, the explosion peak pressure and the propagation speed decrease from 8 to 4MPa and from 200 to 80m/s, respectively.

This result shows that as void fraction is larger, the explosion propagation is slower and the peak pressure is lower. But, it is observed that the coolant velocity is higher. Thus, as void fraction is larger, coolant velocity is larger but the explosion intensities are milder. In explosion propagation, the mixture flow may be induced by its compressibility and therefore flow velocity may be large in more compressible mixture with larger void fractions. But, the explosion propagation speed and pressure become smaller because pressure loss is larger due to the larger compression of the mixture.

were carried out for sensitivity studies on the important parameters in the initial conditions and the constitutive relations. Table 2 represents the explosion peak pressure and average propagation speed with this sensitivity studies. All parameters have an influence on explosions nevertheless its importance are different.

4.3.1. Initial Void Fraction, ε_v

4.3.2. Initial Fuel Fraction, ε_f

As the fuel volume fraction is lower, the explosion

intensity will be weaker. This makes a sense because the amount of fuel melt is the direct energy source for vapor explosions. But, the current calculations with the various fuel fractions do not show the clear results.

It is also observed that when the fuel fraction is low, milder explosion propagation occurs under relatively large vapor fraction(0.2). In case that the fuel and vapor fractions are all low, the fuel is cooled by large amount of liquid coolant and no explosion occurs.

4.3.3. Fragmentation Rate Constant, C_{frag}

C_{frag} has significant effects on the explosion propagation. In small C_{frag} (0.5) the explosion does not occur. As C_{frag} is larger, the propagation speed, the peak pressure, the mixture velocities, and the fragmentation rate are all increase. When C_{frag} is specified with 2.0, the peak pressure is over 15 MPa and the propagation speed is 500m/s. Thus, the fragmentation play an important role of vapor explosion propagation.

In the vapor explosion modeling, the used fragmentation model is not physically complete because the formulation is based upon the experiments with 2-fluid motion, but the vapor explosion have four-components. C_{frag} may be used as a controlling factor to adjust the resulting errors due to this fragmentation equations. It is desirous that the constant, C_{frag}, should be eliminated by further studies.

4.3.4. Heat Transfer Functions Between Liquid Coolant and Vapor, R_{ul}

In our model the liquid coolant and vapor have the different energy equations and the thermodynamic non-equilibrium may be admitted. All heat from fuel and debris is added to liquid phases, and phase change plays a role of making the coolant thermodynamic equilibrium states.

But the real phenomena are different one that the vapor phase will be heated by fuel and debris and high heat transfer between the liquid and vapor occurs. Though this can be revised by relaxation time(τ) because the real phenomena are not mathematically formulated yet, this makes it difficult to apply the EOS due to the worst non-equilibrium and as a result solution becomes unstable. Okano[15] tries to overcome this weakness by introducing the high heat transfer coefficient between the liquid and vapor coolant.

For the R_{ul} of from 0 to 10^7, the peak pressure increase from 8 to 13 MPa and the propagation speed is constant as 200m/s. With an appropriate coefficient(10^7), good results are obtained and the liquid and vapor maintain thermal equilibrium, but with a larger one(10^9) no explosion propagation is done.

4.3.5. Phase Change Relaxation Time, τ

When τ is 0.1 ms ~10 ms, the peak pressure increases from 7 to 9 MPa and the propagation speed is not varied with 200m/s. τ effects mainly exist in the volume fraction change by phase change.

With the results, τ effects on the explosion intensities could be neglected. But, τ beyond some range(0.5~10ms) is not appropriate in the simulation of the explosion propagation. With τ of 0.1ms, the iteration is not converged. This may be resulted from the current calculation time step.

The relaxation time, τ, is not a quantified value and must be carefully selected as time step. Thus, current phase change models have some limitations and must be further studied.

4.3.6. Drag Coefficient, C_D

When C_D has a value of from 1.0 to 4.0, the peak pressure and the propagation speed all decrease from 10 MPa to 5 MPa and from 250m/s to 150m/s. It is easily known that as C_D is larger, the relative velocity is smaller and the peak pressure decreases. Near the shock front the coolant velocity decrease as C_D is larger. Thus, fragmentation rate decreases and explosion intensities are milder.

5. Conclusions

For the numerical simulation of vapor explosion propagation, the TRACER computer code has been developed, which contains a two-dimensional, transient, multi-phase formulation of the four fluid phases of melt drop, fragmented debris, liquid coolant, and vapor coolant. A set of constitutive relations for melt fragmentation, coolant phase-change, and heat and momentum exchanges are incorporated. For simplicity but with reasonable approximations, the model currently solves two momentum equations for the melt drop and the coolant. The later equations for the coolant liquid and vapor are solved separately with a uniquely formulated equation of state for water.

Base calculations are presented for tin/water explosions with the initial conditions in Table 1(A). The results show that the model predicts the explosion propagation speed and peak pressure in a reasonable degree although the quantitative agreement relies strongly on the parameters in the constitutive relations. The comparison with Baines' experimental data shows that a reasonable qualitative agreement although the current model must be advanced to better predict explosion pressures.

A set of calculations for sensitivity studies on these parameters have identified the important initial conditions and relations which must be improved in a great detail. These are melt fragmentation rate, momentum exchange functions and coolant phase-change model as well as equation of state for water which allows non-equilibrium of coolant liquid and vapor. Also local vapor fractions and melt fractions are shown the important initial conditions which must be provided accurately. The importance order of these parameters by the sensitivity studies is shown in Table 3. The order is obtained by the variations of explosion intensities(p_{peak} and $\bar{v}_{prop}$) on those of each parameter.

The mathematical formulation presented in this paper will be used as a base model for further developing an accurate numerical analysis tool for evaluating the potential hazard of in-vessel and ex-vessel fuel-coolant interactions during nuclear severe accidents. Such an effort must include development and improvement of the key physical models as well as validation of the model with experimental data of various material pairs and geometry when it becomes available.

Table 3. Importance Order of Selected Parameters

Parameter	Initial Value (±100%)	P_{peak} (MPa)	$\bar{V}_{prop}$ (m/sec)	Order
ε_v	0.1	8±15%	200±40%	3
α_f	0.4	8±N%	200±N%	2
C_{frag}	1.0	6±150%	200±150%	1
R_{vl}	10^3	10±25%	200±0%	5
τ	1.0	8±15%	200±0%	6
C_D	2.0	8±25%	200±25%	4

Nomenclature

C_D = Drag Coefficient
c_p = Specific Heat
c_{pv} = Specific Heat of Vapor Coolant
c_{frag} = Fragmentation Rate Coefficient
E_f = Emissivity of Fuel Particles
F_r = Fragmentation Rate
h = Heat Transfer Coefficient
H = Enthalpy
I = Internal Energy
I_{lv} = Latent heat of Coolant
J_e = Boiling Rate
J_c = Condensation Rate
K = Momentum Exchange Function
k = Conductivity
L_f = Fuel Droplet Length Scale
p = Pressure
p_{peak} = Explosion Peak Pressure
r_f = Fuel Droplet Radius
R = Heat Transfer Function

s = Entropy
t = Time
T = Temperature
u = Velocity
$\bar{V}_{prop}$ = Average Explosion Propagation Speed

Greek Symbols

α = Volume Fraction
ε = Void Fraction
ρ = Microscopic Density
r = Ratio of Specific Heats
δ = Kronecker Delta
σ = Stefan-Boltzmann Constant

Superscript and Subscript

c = Coolant(Liquid + Vapor + Debris)
db = Debris
e = Evaporation
f = Fuel Droplet
l = Coolant Liquid
v = Coolant Vapor
s, sat = Saturation
fc = between Fuel and Coolant
vl = between Liquid Coolant and Vapor Coolant

Acknowledgements

This work has been supported by Korea Electric Power Corp. (KEPCO) through Electrical Engineering and Science Research Institute(EESRI).

References

1. G. Long, "Explosion of molten metal in water-causes and prevention," Metals progress, **71,** 107~112 (1957)
2. R.C. Reid, "Rapid Phase Transitions form Liquid to Vapor," Adv. Chem. Eng. **12,** 105~208 (1983)
3. D.L. Katz and C.M. Sliepcevich, "Liquified natural gas/water explosions : cause and effect," Hydrocarbon Process, **50,** 240~244 (1971)
4. S.A. Colgate and T. Sigurgeirsson, "Dynamic mixing of water and lava," Nature, **244,** 552~55 (1973)
5. N. Fujii, "Dynamical Aspects of Explosive Eruption," Proc. Int. Sem. on the Physics of Vapor Explosions, Tomakomai, 1~5, Oct (1993)
6. M.L. Corradini, B.J. Kim and M.D. Oh, "Vapour Explosions in Light water Reactors : a Review of Theory and Modeling," Prog. Nucl. Energy, **22,** 1~117 (1988)
7. S.J. Board, R.W. Hall and R.S. Hall, "Detonation of Fuel Coolant Explosions," Nature, **254,** 319~321 (1975)
8. A. Sharon and S.G. Bankoff, "On the Existence of Steady Supercritical Plane Thermal Explosions," Int. J. Heat Mass Transfer, **24,** 1561~1572 (1981)
9. C. Carachalios, M. Burger and H. Unger, "A Transient Two-Phase model to Describe Thermal Detonations Based on Hydrodynamic Fragmentation," Proc. Int. Meeting on LWR Severe Accident Evaluation, Cambridge, Massachusetts, 28, August −1 September, **1,** 6.8.1−8 (1983)
10. S. Medhekar, M. Abolfadl and T.G. Theofanous, "Triggering and Propagation of Steam Explosions," Nucl. Eng. and Design **126,** 41~49 (1991)
11. D.F. Fletcher, "An Improved Mathematical Model of Melt/Water Detonations-I. Model Formulation and Example Results," Int. J. Heat Mass Transfer, **34,** 2435~2448 (1991)
12. M.F. Young, "IFCI : An Integrated Code for Calculation of all Phases of Fuel-Coolant Interaction," NUREG/CR-5084 (1987)
13. C.C. Chu and M.L. Corradini, "One-Dimensional Transient Fluid Model for Fuel/Coolant Interaction Analysis," Nucl. Sci. Eng., **101,** 48~71 (1989)
14. J. Tang and M. L. Corradini, "Modeling of the Complete Process of One-dimensional Vapor Explosion," CSNI, Santa Babara, Jan (1993)

15. T. Okano, "One-dimensional Calculations of Melt/Water Detonations based on a Four-fluid Model," Proc. 2nd Int. Conf. on Multipahse Flow '95-Kyoto (1995)
16. M. Ishii, "Thermo-fluid Dynamic Theory of Two-phase Flow," Eyrolles, Paris (1975)
17. Lester Haar, S.G. Jhon and S. K. Gerge, "Thermodynamic and Transport Properties and Computer Programs for Vapor and Liquid States of Water in SI Units," NBS/NRC Steam Tables (1984)
18. W.C. Rivard and M.D. Torrey, "K-FIX : A Computer Program for Transient, Two-dimensional, Two-fluid Flow," LA-NUREG-6623 (1977)
19. M. Baines, "Preliminary measurements of Steam Explosions Work Yields in a Constrained System," Proc. 1st UK National Heat Transfer Conf., Leeds, UK (1984)